Two-gluon exchange model predictions for double Pomeron jet production

Jon Pumplin
Physics and Astronomy Department, Michigan State University, East Lansing, Michigan 48824
(Received 22 December 1994; revised manuscript received 28 April 1995)

I extend the two-gluon exchange picture of elastic scattering, known as the *Low-Nussinov* or *subtractive quark* model, to predict cross sections for double Pomeron exchange processes. In particular, I calculate $p\bar{p} \to p\bar{p}q\bar{q}$ where the $q\bar{q}$ partons will appear as jets separated from the final p and $\bar{p}$ by large gaps in rapidity. The predicted cross section is large enough that this process should be observable at the Fermilab Tevatron and at the CERN Large Hadron Collider. It can be distinguished from the background of ordinary jet production by an absence of particles produced in the gap regions.

PACS number(s): 13.87.Ce, 12.39.−x, 12.40.Nn, 13.85.Ni

I. INTRODUCTION

The exchange of a gluon is the simplest interaction between two hadrons in QCD. It corresponds, via s-channel unitarity, to an elastic amplitude dominated by exchange of two-gluons in a state with vacuum quantum numbers — in particular, a color singlet. This provides a simple model, known as the Low-Nussinov model [1, 2], for the Pomeron that governs diffractive scattering at high energy. The energy dependence of the model (s^1 in the amplitude) is close to the observed behavior ($\sim s^{1.08}$ [3, 4]), so the picture is qualitatively reasonable.

In this paper, we extend the Low-Nussinov model to predict cross sections for double Pomeron exchange (DPE) processes [5–8], which are characterized by two large rapidity gaps [9, 10]. It has been suggested [5] that these processes will be observable at the Fermilab Tevatron, and it is important to try to predict their cross sections. DPE will also be an interesting subject for study at the CERN Large Hadron Collider (LHC) ($\sqrt{s} \cong 14$ TeV).

We will focus on $q\bar{q}$ jet production in $p\bar{p}$ scattering, where the final state contains only the two jets and a p and $\bar{p}$ that carry $\gtrsim 95\%$ of their original momenta. The final p and $\bar{p}$ have transverse momenta $\lesssim 1$ GeV, putting them too close to the beam directions (pseudorapidity $|\eta| > 7$) to be seen with present detectors. The absence of particles produced outside the two jets (in Lego variables η and ϕ), except in the region between them because of soft QCD radiation, contrasts strikingly to ordinary events, especially those with a hard scattering, so the signature of DPE-produced jets will be unmistakable. Meanwhile, the hard scattering amplitude is under control in perturbative QCD, so no new parameters are added to the Low-Nussinov picture to make the prediction.

To calculate two-gluon exchange, we need a model for the internal color structure of the hadrons to which the two-gluon system couples. In this paper, the scattering hadrons are taken to be $q\bar{q}$ bound states of effective "quarks" that have spin zero and couple to the hadrons by a point coupling. One might of course prefer qqq for the wave function of a baryon, and additional $q\bar{q}$ pairs and gluons are certainly present in wave functions for small momentum transfer. Our simple model may nevertheless be adequate, since only the distribution of color in the hadron is significant for the calculation, and that can be modeled correctly by adjusting parameters to fit elastic scattering. Indeed, only the distribution of color as a function of impact parameter really matters since the spin 1 gluon "sees" quarks equally, regardless of their longitudinal momentum. This justifies the simplicity of using spin 0 quarks. We will also try an exponentially falling model for the wave function, which is more realistic. The model dependence will be assessed by comparing results obtained using the two different wave function types, with a range of choices for their parameters.

Higher-order effects such as interaction between the exchanged gluons must be important at some level and is evidenced by the deviation from constant total cross sections as a function of energy. Interactions could even build a rather conventional Regge trajectory for the Pomeron, with physical glueball states on it at positive t, as Landshoff has emphasized recently [4]. More-than-two-gluon exchange contributions are also not negligible, as can be estimated by eikonalizing the two-gluon amplitude [2]. (The contribution beginning with four-gluon exchange has sometimes also been called double Pomeron exchange [11]. It must not be confused with the definition of DPE used here.) We will neglect these effects both for elastic scattering and jet production. Fitting the model parameters to elastic scattering should reduce the consequences of this approximation.

In spite of its simplicity, it is worthwhile to see what this model has to say about jet production in double Pomeron exchange, which has not until now been calculated, even though more exotic DPE processes of heavy quark [7] and Higgs boson [12] production have been. The calculation will be presented in considerable detail to make clear how it could be applied to other double-diffractive processes. The model could also be applied to hard scattering with the exchange of just one soft Pomeron, i.e., hard scattering in diffractive dissociation. Examples for study would be $\gamma p \to q\bar{q}p$, which can be observed at the DESY ep collider HERA and has been calculated in somewhat different models [13–15]; and single-diffractive production of $W^{\pm}$ which has been

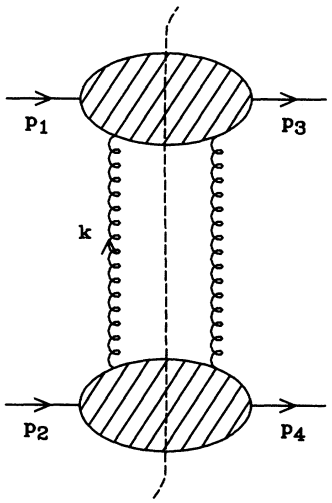

FIG. 1. Two-gluon exchange ("Low-Nussinov") model for the elastic amplitude. The dashed line denotes an s-channel discontinuity.

looked for by the Collider Detector at Fermilab Collaboration (CDF) [16].

An additional theoretical motivation for this work is that the two-gluon exchange picture provides an explicit model for a "direct," "coherent," or "lossless" contribution [17, 18], in which the full energy of the Pomeron is available for hard scattering. From a theoretical standpoint, such contributions are interesting because they violate the QCD factorization rules that have been established for inclusive processes and that are often assumed without proof for the diffractive subset of final states [19, 20]. They appear as an effective "superhard" term $\propto \delta(x-1)$ in the phenomenological parton distribution of the Pomeron. Suggestive experimental evidence for a coherent contribution has been seen by UA8 [21].

II. ELASTIC SCATTERING

The Pomeron is believed to arise from diffractive physics, i.e., to be an s-channel unitarity phenomenon.

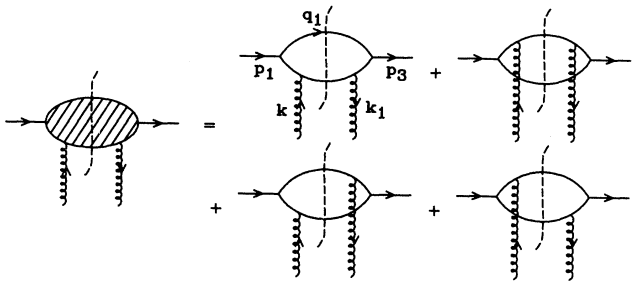

FIG. 2. Quark model for the hadronic discontinuity in Fig. 1.

We therefore want the imaginary part of the two-gluon exchange amplitude, which can be calculated for elastic scattering from the discontinuity illustrated in Fig. 1:

$$\mathcal{M} = \frac{-8}{2i(2\pi)^4} \int \frac{d^4k}{(k^2 - m_g^2)\,[(k+p_1-p_3)^2 - m_g^2]} \times D_{\mu\nu}(p_1, k \to p_3, k+p_1-p_3) \times D_{\mu\nu}(p_2, -k \to p_4, -k+p_2-p_4)\,. \tag{1}$$

Note that the imaginary part is conveniently found by cutting the diagram into two pieces through the possible physical intermediate states. Alternatively, one could calculate the amplitude as a Feynman diagram, in which case there would be an additional diagram in which the two-gluons cross each other. The real part would cancel between these diagrams because the amplitude has even signature and energy dependence $\propto s^1$.

Equation (1) contains a factor 8 from the sum over gluon colors. A finite mass m_g is included in the gluon propagators to suppress contributions from long distance, as an approximation to color confinement. (An alternative modification of the gluon propagator is discussed in Ref. [22].)

Our model for the discontinuity of the gluon-hadron amplitude, illustrated in Fig. 2, is

$$D_{\mu\nu}(p_1, k \to p_3, k+p_1-p_3) = \frac{g^2 G^2}{2} \int \frac{d^4q_1}{(2\pi)^4}\,[2\pi i\,\delta(q_1^2 - m^2)]\,[2\pi i\,\delta(q_2^2 - m^2)] \times \left[\frac{(p_1 - q_1 + q_2)_\mu}{(p_1 - q_1)^2 - m^2} - \frac{(p_1 - q_2 + q_1)_\mu}{(p_1 - q_2)^2 - m^2}\right] \times \left[\frac{(p_3 - q_1 + q_2)_\nu}{(p_3 - q_1)^2 - m^2} - \frac{(p_3 - q_2 + q_1)_\nu}{(p_3 - q_2)^2 - m^2}\right], \tag{2}$$

where $q_2 = k + p_1 - q_1$, and g and G are couplings of the scalar quark to a gluon and to the hadron. An overall factor $\frac{1}{2}$ from color is included, although it is not actually significant because the coupling strength $g^2 G^2$ is taken as a free parameter of the model.

In view of the δ functions, Eq. (2) appears to be a two-dimensional integral. In the high energy limit, however, one of the δ functions can be reserved to apply to the d^4k integral in Eq. (1), leaving a three-dimensional integral. To see this, introduce the light-cone coordinates $p_\pm = (p_0 \pm p_z)/\sqrt{2}$ and work in a Lorentz frame such as the center of mass, where $p_{1+} \cong p_{3+}$ and $p_{2-} \cong p_{4-}$ are large with $s = (p_1 + p_2)^2 \cong 2\,p_{1+}\,p_{2-}$. Then $d^4q = d^2q_\perp\,dq_+\,dq_-$. Introduce

$x_1 = q_{1+}/p_{1+}$ and $x_2 = q_{2+}/p_{1+}$ and use $\delta(q_1^2 - m^2) = \delta(2\,q_{1+}\,q_{1-} - q_{1\perp}^2 - m^2)$ to do the q_{1-} integral. The other δ function becomes

$$\delta(q_2^2 - m^2) \cong \frac{\delta(k_-)}{2\,q_{2+}} \cong \frac{\delta(p_1 \cdot k)}{x_2} \tag{3}$$

in the high energy limit, and we obtain

$$D_{\mu\nu}(p_1, k \to p_3, k + p_1 - p_3) = (p_1)_\mu\,(p_1)_\nu\,\delta(p_1 \cdot k)\,T(\vec{k}_\perp, (\vec{p}_3 - \vec{p}_1)_\perp)\ , \tag{4}$$

where

$$\begin{aligned} T(\vec{k}_\perp, (\vec{p}_3 - \vec{p}_1)_\perp) = \frac{-g^2\,G^2}{8\,\pi^2} \int_0^1 dx_1 \int_0^1 dx_2\, x_1\,x_2\,\delta(1 - x_1 - x_2) \int d^2\vec{q}_{1\perp} \\ \times \left[\frac{1}{(\vec{q}_{1\perp} - x_1\,\vec{p}_{1\perp})^2 + \tilde{m}^2} - \frac{1}{(\vec{q}_{2\perp} - x_2\,\vec{p}_{1\perp})^2 + \tilde{m}^2}\right] \\ \times \left[\frac{1}{(\vec{q}_{1\perp} - x_1\,\vec{p}_{3\perp})^2 + \tilde{m}^2} - \frac{1}{(\vec{q}_{2\perp} - x_2\,\vec{p}_{3\perp})^2 + \tilde{m}^2}\right]\ . \end{aligned} \tag{5}$$

Here $\vec{q}_{2\perp} = (\vec{p}_1 + \vec{k} - \vec{q}_1)_\perp$, and $\tilde{m}^2 = m^2 - x_1 x_2 M^2$ with M the mass of the hadron and m the mass of the "quark." We have ignored the differences between $(p_1)_\mu\,(p_1)_\nu$, $(p_1)_\mu\,(p_3)_\nu$, and $(p_3)_\mu\,(p_3)_\nu$, which are nonleading in s.

The transverse momentum integrations can be carried out to obtain

$$T(\vec{k}_\perp, \vec{\Delta}_\perp) = F(\vec{k}_\perp, \vec{\Delta}_\perp) - F(\vec{0}, \vec{\Delta}_\perp)\ , \tag{6}$$

where

$$F(\vec{k}_\perp, \vec{\Delta}_\perp) = \frac{g^2\,G^2}{4\,\pi^2} \int_0^1 \frac{dx}{x\,(1-x)} \int d^2\vec{q}_\perp \left[\frac{\vec{q}_\perp^{\,2} + m^2}{x\,(1-x)} - M^2\right]^{-1} \left[\frac{(\vec{q}_\perp + \vec{k}_\perp - x\vec{\Delta}_\perp)^2 + m^2}{x\,(1-x)} - M^2\right]^{-1} \tag{7}$$

$$= \frac{g^2\,G^2}{2\,\pi} \int_0^1 dx\,x\,(1-x)\,\frac{1}{AB}\,\ln\frac{B+1}{B-1} \tag{8}$$

with $A = (\vec{k}_\perp - x\vec{\Delta}_\perp)^2$ and $B = \sqrt{1 + 4\tilde{m}^2/A}$. The remaining integration over quark momentum fraction x can be done numerically by Gauss-Legendre integration.

A more realistic model can be made by replacing the two energy denominator factors of the form $[X - M^2]^{-1}$ in Eq. (7) by exponentials $\propto e^{-\beta X}$. This leads to

$$F(\vec{k}_\perp, \vec{\Delta}_\perp) = N \int_0^1 dx\,\exp\{-\beta\,[\,(\vec{k}_\perp - x\vec{\Delta}_\perp)^2 + 4\,m^2\,]/2\,x\,(1-x)\}\ , \tag{9}$$

where the three constants β, m, and the normalization N parametrize the wave function in place of the point-coupling model parameters. The exponential form mimics the fragility of actual hadrons at low momentum transfer, which is displayed by the approximately exponential falloff of elastic amplitudes at small $-t$. The structure of Eq. (9) can be seen better by writing it as

$$F(\vec{k}_\perp, \vec{\Delta}_\perp) = N \int_0^1 dx\,\exp\{-(\beta/2)\,[\,(k_1^2 + 4m^2)/x + (k_2^2 + 4m^2)/(1-x) - \vec{\Delta}_\perp^{\,2}\,]\}\ , \tag{10}$$

where $k_1^2 = \vec{k}_\perp^{\,2}$ and $k_2^2 = (\vec{\Delta}_\perp - \vec{k}_\perp)^2$ are the squared momentum transfers carried by each gluon. A saddle-point approximation to Eq. (10) is convenient for speeding up numerical calculations:

$$F(\vec{k}_\perp, \vec{\Delta}_\perp) \cong N \sqrt{\frac{2\pi ab}{\beta}}\,(a+b)^{-2}\,e^{-(\beta/2)\,[\,(a+b)^2 - \vec{\Delta}_\perp^{\,2}\,]}\ , \tag{11}$$

where $a = \sqrt{k_1^2 + 4m^2}$ and $b = \sqrt{k_2^2 + 4m^2}$.

Returning to Eqs. (1)–(4), we have

$$\mathcal{M} = \frac{i\,s}{8\,\pi^4} \int \frac{d^2\vec{k}_\perp\,[T(\vec{k}_\perp, \vec{\Delta}_\perp)]^2}{(\vec{k}_\perp^{\,2} + m_g^2)\,[(\vec{k}_\perp - \vec{\Delta}_\perp)^2 + m_g^2]}\ , \tag{12}$$

with $\vec{\Delta}_\perp^{\,2} \cong -(p_1 - p_3)^2 = -t$ the momentum transfer. The $\vec{k}_\perp$ integration can be done numerically.

We have three models for the proton wave function, given by Eqs. (8), (10), and (11), with the latter two equivalent except in computational convenience. On physical grounds, we estimate $m = 0.5$ (or 0.3) and $m_g = 0.3$ (or 0.14 or 1.0) in GeV = 1 units, with the al-

ternatives representing an estimate of the possible range.

The model amplitude is proportional to s^1 as expected for spin 1 exchange. It thus describes an energy-independent total cross section and elastic $d\sigma/dt$. To choose the remaining two parameters in each model, we fit the elastic and total cross sections to $\sigma_{\rm tot} = 65$ mb and $\sigma_{\rm el}/\sigma_{\rm tot} = 0.207$, which are based on a fit [23] to $p\bar{p}$ elastic scattering data [24] at $\sqrt{s} = 546$ GeV. The parameter values are shown in Table I.

The parameters of the point-coupling model [Eq. (8)] are such that $2m$ is very close to M. This can be understood using the uncertainty principle: the large spatial extent of the proton, which is responsible for the large elastic slope, is reproduced in the model by the possibility of nearly on-shell dissociation of the proton into its constituents. A choice like $m = M = m_g = 0.3$, suggested in preliminary work by Berera [25], for example, would instead make $\sigma_{\rm el}/\sigma_{\rm tot} = 0.87$, which is much too large. Equivalently, but independent of the normalization, it would make the average elastic slope $\sigma_{\rm tot}^2/16\pi\sigma_{\rm el}$ equal to $3.8\,{\rm GeV}^{-2}$ instead of $16.0\,{\rm GeV}^{-2}$.

The exponentially falling wave function models [Eqs. (10) and (11)] reproduce the actual shape of $d\sigma/dt$ much better than the point-coupling model. These two models are very similar, since the second is just a saddle-point approximation to the first, with parameters chosen to give the same $\sigma_{\rm tot}$ and $\sigma_{\rm el}$. Our smallest choice $m_g = 0.14$ begins to have a slope at $t = 0$ that is too steep, since the slope diverges in the limit $m_g \to 0$.

The hadronic discontinuity modeled by Fig. 2 is actually a function of three scalar variables, say $\vec{k}_{1\perp}^{\,2}$, $\vec{k}_{2\perp}^{\,2}$, and $(\vec{k}_{1\perp} + \vec{k}_{2\perp})^2$. Tuning the model parameters to fit the t dependence of elastic scattering may therefore not be sufficient to determine it. (The ambiguity could be reduced by also fitting the electromagnetic form factor [2].) However, we will find that the predictions are not extremely sensitive to the form of the model.

Some important aspects of Eq. (12) are especially clear in the forward direction, where it reduces to

$$\sigma_{\rm tot} = \frac{1}{8\pi^4}\int d^2\vec{k}_\perp \left(\frac{F(\vec{0},\vec{0}) - F(\vec{k}_\perp,\vec{0})}{\vec{k}_\perp^{\,2} + m_g^2}\right)^2 . \quad (13)$$

The factor $F(\vec{0},\vec{0}) - F(\vec{k}_\perp,\vec{0})$ represents the response of the hadronic wave function to gluon momentum transfers of $\vec{k}_\perp$ and $-\vec{k}_\perp$. $F(\vec{0},\vec{0})$ comes from the "diagonal" diagrams in Fig. 2, where both gluons hit the same quark line so there is no $\vec{k}_\perp$ dependence from the wave function. $F(\vec{k}_\perp,\vec{0})$ comes from the "off-diagonal" diagrams in which the gluons hit different quarks.

Equation (13) has two different momentum scales: one associated with the gluon propagator and one associated with the hadronic wave function. The overall dependence on $\vec{k}_\perp$ is set by the fit to elastic scattering, but the relative contributions are not well determined.

First, consider the parameters in Table I for Eq. (10) with the smallest assumed $m_g = 0.14 \cong m_\pi$, which corresponds to relatively long-range color confinement. We find $F(\vec{0},\vec{0}) - F(\vec{k}_\perp,\vec{0}) \approx F(\vec{0},\vec{0})\,(1 - e^{-11\vec{k}_\perp^{\,2}})$. With these parameters, the cancellation between diagonal and off-diagonal terms is extremely important: omitting the off-diagonal term would increase $\sigma_{\rm tot}$ by a factor > 5. Meanwhile, the gluon mass is rather unimportant: even setting it to zero would increase $\sigma_{\rm tot}$ by only a factor of 1.6. To emphasize the importance of cancellation be-

TABLE I. Parameters of the model and predicted C_a.

Model	m	m_g	Other parameters		$C_a = C_b$
Eq. (8)	0.5	0.14	$M = 0.9818$	$g^2G^2 = 2.67$	2.7×10^{-3}
Eq. (8)	0.3	0.14	$M = 0.5638$	$g^2G^2 = 1.976$	2.2×10^{-3}
Eq. (8)	0.5	0.30	$M = 0.9868$	$g^2G^2 = 2.795$	1.2×10^{-3}
Eq. (8)	0.3	0.30	$M = 0.5741$	$g^2G^2 = 2.011$	9.4×10^{-4}
Eq. (8)	0.5	1.0	$M = 0.9916$	$g^2G^2 = 4.671$	6.7×10^{-5}
Eq. (8)	0.3	1.0	$M = 0.5840$	$g^2G^2 = 3.285$	7.0×10^{-5}
Eq. (10)	0.5	0.14	$\beta = 5.869$	$N = 3.24 \times 10^7$	2.8×10^{-3}
Eq. (10)	0.3	0.14	$\beta = 5.301$	$N = 7.50 \times 10^3$	2.3×10^{-3}
Eq. (10)	0.0	0.14	$\beta = 2.378$	$N = 7.23 \times 10^1$	9.2×10^{-4}
Eq. (10)	0.5	0.30	$\beta = 6.715$	$N = 2.51 \times 10^8$	1.4×10^{-3}
Eq. (10)	0.3	0.30	$\beta = 6.222$	$N = 2.05 \times 10^4$	1.1×10^{-3}
Eq. (10)	0.0	0.30	$\beta = 3.487$	$N = 8.91 \times 10^1$	8.4×10^{-4}
Eq. (10)	0.5	1.0	$\beta = 7.682$	$N = 4.65 \times 10^9$	5.1×10^{-5}
Eq. (10)	0.3	1.0	$\beta = 7.358$	$N = 1.24 \times 10^5$	4.4×10^{-5}
Eq. (10)	0.0	1.0	$\beta = 5.261$	$N = 2.14 \times 10^2$	2.8×10^{-4}
Eq. (11)	0.5	0.14	$\beta = 5.797$	$N = 2.65 \times 10^7$	2.8×10^{-3}
Eq. (11)	0.3	0.14	$\beta = 4.944$	$N = 4.89 \times 10^3$	2.1×10^{-3}
Eq. (11)	0.5	0.30	$\beta = 6.659$	$N = 2.13 \times 10^8$	1.4×10^{-3}
Eq. (11)	0.3	0.30	$\beta = 5.901$	$N = 1.40 \times 10^4$	1.0×10^{-3}
Eq. (11)	0.5	1.0	$\beta = 7.638$	$N = 4.06 \times 10^9$	4.9×10^{-5}
Eq. (11)	0.3	1.0	$\beta = 7.098$	$N = 9.04 \times 10^4$	4.1×10^{-5}

tween contributions in which the gluons couple to the same or to different quarks, which follows from color neutrality of the complete hadron, this picture has been called the *subtractive quark model* [2], in contrast to the pre-QCD additive quark point of view.

Now consider instead the parameters in Table I for Eq. (10) with the largest assumed value $m_g = 1.0\,\mathrm{GeV}$, which corresponds to very short-range confinement. We find $F(\vec{0},\vec{0}) - F(\vec{k}_\perp,\vec{0}) \approx F(\vec{0},\vec{0})\,(1-e^{-15\vec{k}_\perp^2})$. With this choice of parameters, the off-diagonal term is quite unimportant: omitting it would increase $\sigma_{\rm tot}$ by only 10%. This point of view in which the diagonal terms are dominant corresponds to the additive quark picture advocated by Donnachie and Landshoff [4, 26].

We will find that the DPE predictions are somewhat different for the different choices of m_g, so DPE measurements might eventually be used to decide the correct point of view.

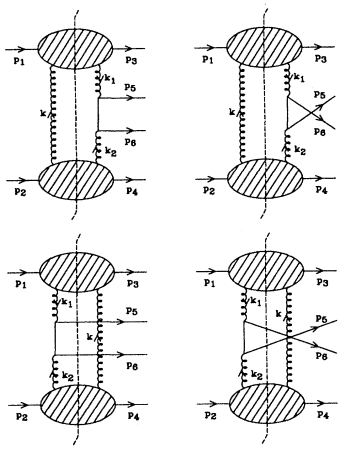

FIG. 3. Two gluon exchange model for double Pomeron exchange production of $q\bar{q}$ jets.

III. DPE PRODUCTION OF $Q\bar{Q}$ JETS

Figure 3 shows a natural extension of the Low-Nussinov model to describe $q\bar{q}$ jet production in DPE. These diagrams can be expected to dominate all other contributions because the hadronic discontinuities $D_{\mu\nu}$ contain phase-coherent sums over physical states, like their counterparts in elastic scattering. As in the case of elastic scattering, a diagrammatic calculation would include crossed graphs that individually generate real parts which cancel in the sum. The discontinuity method is simpler as well as being more intuitively related to s-channel unitarity.

The absorptive part of the amplitude is

$$\mathcal{M}_{q\bar{q}} = \frac{i\,g^2}{2(2\pi)^4}\int d^4k\,\frac{1}{(k^2-m_g^2)\,(k_1^2-m_g^2)\,(k_2^2-m_g^2)}[D_{\beta\mu}(p_1,k\to p_3,k_1)\,D_{\beta\nu}(p_2,-k\to p_4,k_2)$$
$$+D_{\mu\beta}(p_1,-k_1\to p_3,-k)\,D_{\nu\beta}(p_2,-k_2\to p_4,k)]\bar{u}(p_5)\left[\frac{\gamma_\mu\,\gamma\cdot(p_5-k_1)\,\gamma_\nu}{(p_5-k_1)^2}+\frac{\gamma_\nu\,\gamma\cdot(p_5-k_2)\,\gamma_\mu}{(p_5-k_2)^2}\right]v(p_6)\,, \qquad (14)$$

where $k_1 = p_1 - p_3 + k$ and $k_2 = p_2 - p_4 - k$. Note that we use true spin 1/2 massless quarks here, in contrast to the effective "quarks" used in the wave function model. Equation (4) reduces this to an integral over transverse momentum, and the contributions from the two sets of diagrams in Fig. 3 are equal in view of the symmetry $T(\vec{k}_\perp,\vec{\Delta}_\perp) = T(\vec{\Delta}_\perp - \vec{k}_\perp,\vec{\Delta}_\perp)$. This leads to

$$\mathcal{M}_{q\bar{q}} = \frac{i\,g^2}{16\,\pi^4}\int d^2\vec{k}_\perp\,f(\vec{k}_\perp)\,A_{q\bar{q}}, \qquad (15)$$

$$f(\vec{k}_\perp) = \frac{T(\vec{k}_\perp,\vec{p}_{3\perp})\;T(-\vec{k}_\perp,\vec{p}_{4\perp})}{(\vec{k}_\perp^{\,2}+m_g^2)\,(\vec{k}_{1\perp}^{\,2}+m_g^2)\,(\vec{k}_{2\perp}^{\,2}+m_g^2)}, \qquad (16)$$

$$A_{q\bar{q}} = \bar{u}(p_5)\left[\frac{\gamma\cdot p_1\,\gamma\cdot(p_5-k_1)\,\gamma\cdot p_2}{(p_5-k_1)^2}+\frac{\gamma\cdot p_2\,\gamma\cdot(p_5-k_2)\,\gamma\cdot p_1}{(p_5-k_2)^2}\right]v(p_6)\,, \qquad (17)$$

where we set $\vec{p}_{1\perp} = \vec{p}_{2\perp} = 0$ for incoming particles in the $\pm\hat{z}$ direction.

To compute $|\mathcal{M}_{q\bar{q}}|^2$, first compute $\sum A^*_{q\bar{q}}(k')\,A_{q\bar{q}}(k)$ where the sum is over q and $\bar{q}$ helicities and k' is an integration variable independent from k. Neglect nonleading powers in s by dropping p_{1-}, k_{1-}, p_{2+}, k_{2+}. Let

$$\vec{Q}_\perp = (\vec{p}_{5\perp} - \vec{p}_{6\perp})/2\,, \qquad (18)$$

where $|\vec{Q}_\perp|$ is essentially the transverse momentum of each jet since $\vec{p}_{5\perp} + \vec{p}_{6\perp} = -\vec{p}_{3\perp} - \vec{p}_{4\perp}$, with $|\vec{p}_{3\perp}|$ and $|\vec{p}_{4\perp}|$ limited to $\lesssim 1\,\mathrm{GeV}$ by the proton wave function. The transverse momentum in the loop integration is also limited by the proton wave function, so $Q_\perp$ is large compared to all other transverse momenta. Keeping only the leading power in $Q_\perp$ gives

$$\sum A^*_{q\bar{q}}(k')\,A_{q\bar{q}}(k) = \frac{40\,s^2}{3\,Q_\perp^4\,\cosh^4\delta}\,[a(k')\,a(k)\,\cosh^2\delta + b(k')\,b(k)\,\sinh^2\delta]\,, \qquad (19)$$

where

$$\delta = (y_5 - y_6)/2\,, \qquad (20)$$

and

$$a(k) = (k_1)_x\,(k_2)_y + (k_1)_y\,(k_2)_x, \qquad (21)$$
$$b(k) = (k_1)_x\,(k_2)_x - (k_1)_y\,(k_2)_y, \qquad (22)$$

with $\vec{k}_{1\perp} = \vec{k}_\perp - \vec{p}_{3\perp}$, $\vec{k}_{2\perp} = -\vec{k}_\perp - \vec{p}_{4\perp}$, and $\vec{Q}_\perp$ taken to be in the $\hat{x}$ direction. Equation (19) includes a factor of $\frac{16}{3}$ from color and a factor of 5 to sum over the quark jet flavors d, u, s, c, b. (Double-diffractive *top* production

will be a welcome newcomer at the LHC.)

The cross section is

$$\frac{d\sigma}{d^2\vec{p}_{3\perp}\, d^2\vec{p}_{4\perp}\, d^2\vec{Q}_\perp\, dy_5\, dy_6} = \frac{|\mathcal{M}_{q\bar{q}}|^2}{2^{12}\,\pi^8\, s^2}, \tag{23}$$

where y_5 and y_6 are the rapidities of the two jets. Both terms in Eq. (19) contain a function of $\vec{k}'_\perp$ times a function of $\vec{k}_\perp$. Their contributions to $|\mathcal{M}_{q\bar{q}}|^2$ can therefore be computed as absolute squares of integrals over $\vec{k}_\perp$:

$$\frac{d\sigma}{d^2\vec{p}_{3\perp}\, d^2\vec{p}_{4\perp}\, d^2\vec{Q}_\perp\, dy_5\, dy_6} = \frac{\alpha_s^2}{Q_\perp^4\,\cosh^4\delta} \times(c_a\,\cosh^2\delta + c_b\,\sinh^2\delta)\,, \tag{24}$$

where

$$c_a = \frac{10}{3\,(2\pi)^{14}}\left|\int d^2\vec{k}_\perp\, f(\vec{k}_\perp)\, a(\vec{k}_\perp)\right|^2, \tag{25}$$

$$c_b = \frac{10}{3\,(2\pi)^{14}}\left|\int d^2\vec{k}_\perp\, f(\vec{k}_\perp)\, b(\vec{k}_\perp)\right|^2. \tag{26}$$

These results can also be obtained by calculating the individual $q\bar{q}$ helicity amplitudes. The cross sections are equal for helicities $(+1/2\ -1/2)$ and $(-1/2\ +1/2)$, and zero for $(+1/2\ +1/2)$ and $(-1/2\ -1/2)$.

The cross section is independent of overall energy s. The dependence on jet transverse momentum is the usual dimensional $Q_\perp^{-4}$. The dependence on $\delta = (y_5 - y_6)/2$ is such that the two jets are usually separated by $\lesssim 2$ units of rapidity. For large δ, the cross section falls as $e^{-|y_5-y_6|}$ which is dictated by Regge arguments for spin 1/2 exchange. Similarly, there is no dependence on the average rapidity $y_{\rm ave} = (y_5+y_6)/2$ of the jet pair because the gluons have spin 1.

In the special case where both leading particles have zero transverse momentum $\vec{p}_{3\perp} = \vec{p}_{4\perp} = 0$, the cross section is found to be zero as a result of the azimuthal angle integrations in Eqs. (25) and (26). This implies strong correlations between the transverse momenta of the leading particles. A "Regge factorization" assumption, whereby the cross section is a product of factors for emission of Pomerons by the fast particles times a cross section for two-Pomeron scattering, would be incorrect. It also implies that it is dangerous to estimate the DPE cross section on the basis of the pure forward direction, as is done in somewhat different models for heavy quark [7] and Higgs boson [12] production.

Integrating over the transverse momenta of both quasielastically scattered p and $\bar{p}$, since these cannot be observed in current experiments, gives

$$\frac{d\sigma}{d^2\vec{Q}_\perp\, dy_5\, dy_6} = \frac{\alpha_s^2}{Q_\perp^4\,\cosh^4\delta}\,(C_a\,\cosh^2\delta + C_b\,\sinh^2\delta)\,. \tag{27}$$

When c_a and c_b are integrated over the azimuthal angles of $\vec{p}_{3\perp}$ and $\vec{p}_{4\perp}$, they are found to become equal. *Hence $C_a = C_b$ in Eq. (27).* Results are shown in Table I for our various choices of proton wave function and gluon mass. We find $C_a = C_b \approx 1.2\times10^{-3}$ with an uncertainty up or down of a factor of 2.5. Somewhat smaller results than that are found for the rather extreme choice $m_g = 1.0$.

The large $Q_\perp$ limit in Eqs. (19)–(22) was computed with the help of MATHEMATICA [27]. It is interesting to compare it with production of *spin zero* quarks, which is simple enough to work out by hand as follows. The spin 1/2 factors in Eq. (14) are replaced by the likewise gauge-invariant form

$$\frac{(k_1-2p_5)_\mu\,(k_2-2p_6)_\nu}{(k_1-p_5)^2} + \frac{(k_1-2p_6)_\mu\,(k_2-2p_5)_\nu}{(k_1-p_6)^2} + 2\delta_{\mu,\nu}\,. \tag{28}$$

Equation (17) is replaced by

$$A_{\rm spin\,0} = \frac{s\,(1-\alpha\beta)}{(1+\alpha)\,(1+\beta)}\,, \tag{29}$$

where

$$\alpha = (\vec{k}_1-\vec{p}_5)^2_\perp/2\,p_{5-}\,p_{6+},\qquad \beta = (\vec{k}_1-\vec{p}_6)^2_\perp/2\,p_{5+}\,p_{6-}\,. \tag{30}$$

It suffices to approximate $\alpha \cong e^{2\delta}$ and $\beta \cong e^{-2\delta} \Rightarrow (1+\alpha)\,(1+\beta) \cong 4\cosh^2\delta$ in the denominator. Terms of order $1/Q_\perp^2$ must be kept in the numerator because $\alpha\beta$ is close to 1, leading to

$$A_{\rm spin\,0} = \frac{s}{2\,Q_\perp^2\,\cosh^2\delta}\left(2\,\hat{Q}_\perp\cdot\vec{k}_{1\perp}\;\hat{Q}_\perp\cdot\vec{k}_{2\perp} - \vec{k}_{1\perp}\cdot\vec{k}_{2\perp}\right) \tag{31}$$

$$= \frac{s}{2\,Q_\perp^2\,\cosh^2\delta}\,(k_{1x}\,k_{2x} - k_{1y}\,k_{2y})\,, \tag{32}$$

where the final form is for $\vec{Q}_\perp$ in the $\hat{x}$ direction. The dependence on $\vec{k}_{1\perp}$ and $\vec{k}_{2\perp}$ is the same as in Eq. (22), so the cross section again goes to zero in the double forward limit $\vec{p}_{3\perp} = \vec{p}_{4\perp} = 0$. The dependence of the cross section on rapidity is $(\cosh\delta)^{-4}$, which falls as $e^{-2|y_5-y_6|}$ for large separation as required by Regge theory for spin 0 exchange.

IV. EXPERIMENTAL CONSIDERATIONS

A measurement that could be made with the CDF or DØ detectors at Fermilab ($\bar{p}p$ at $\sqrt{s} = 1800\,\text{GeV}$) would require two jets in the central region of pseudorapidity, say $|\eta_5|, |\eta_6| < 1.5$. Defining the jets using a cone radius of 0.7 would leave regions of at least $2.2 < |\eta| < 4.2$ in the two "end-cap" parts of the detector, to observe the *absence* of produced hadrons that distinguishes DPE from ordinary hard scattering.

The fraction of longitudinal momentum retained by the forward incident proton is $X_1 \cong p_{3+}/p_{1+} \cong 1 - (p_{5+}+p_{6+})/p_{1+} \cong 1 - (e^{\eta_5}+e^{\eta_6})Q_\perp/\sqrt{s}$. Similarly, $X_2 \cong 1-(e^{-\eta_5}+e^{-\eta_6})Q_\perp/\sqrt{s}$ is the fraction of momentum retained by the backward antiproton. Requiring X_1, $X_2 > 0.95$ defines the DPE region as

$$\begin{aligned} |\eta_5| &< 1.5, \\ |\eta_6| &< 1.5, \\ e^{\eta_5} + e^{\eta_6} &< 0.05\sqrt{s}/Q_\perp, \\ e^{-\eta_5} + e^{-\eta_6} &< 0.05\sqrt{s}/Q_\perp . \end{aligned} \tag{33}$$

The predicted DPE cross section for $q\bar{q}$ jets is calculated by integrating Eq. (27) over the region defined by Eq. (33). In doing this, I take $\alpha_s(Q^2) = 12\pi/(23\ln Q^2/\Lambda^2)$ with $\Lambda = 0.2\,\mathrm{GeV}$ and $Q^2 = Q_\perp^2/4$. The result is

$$\sigma = \begin{cases} (3.516\,C_a + 0.632\,C_b)\ \mu\mathrm{b} & \text{for jets with } Q_\perp > 10\,\mathrm{GeV}/c, \\ (0.246\,C_a + 0.040\,C_b)\ \mu\mathrm{b} & \text{for jets with } Q_\perp > 20\,\mathrm{GeV}/c, \\ (0.022\,C_a + 0.002\,C_b)\ \mu\mathrm{b} & \text{for jets with } Q_\perp > 30\,\mathrm{GeV}/c\,. \end{cases} \tag{34}$$

Using $C_a = C_b$ and taking $C_a = 1.2 \times 10^{-3}$ as a typical estimate from Table I gives

$$\sigma = \begin{cases} 4.98\,\mathrm{nb} & \text{for jets with } Q_\perp > 10\,\mathrm{GeV}/c, \\ 0.34\,\mathrm{nb} & \text{for jets with } Q_\perp > 20\,\mathrm{GeV}/c, \\ 0.03\,\mathrm{nb} & \text{for jets with } Q_\perp > 30\,\mathrm{GeV}/c\,. \end{cases} \tag{35}$$

These predictions are uncertain by a factor of 2–3 due to the model dependence indicated by the spread of values for C_a. The final predicted cross sections will be larger because the contribution from gluon jet production is yet to be calculated.

One might expect the cross section to be reduced by the following "$t_{\min}$" effect. The four-momentum transfer to the leading proton is

$$t_1 = (p_1 - p_3)^2 = -[\vec{p}_{3\perp}^{\,2} + (1 - X_1)^2\, m_p^2]/X_1\ , \tag{36}$$

which becomes $-\vec{p}_{3\perp}^{\,2}$ in the $X_1 \to 1$ limit that is assumed in our calculation. To correct for this approximation, the predicted cross section should be reduced by a factor $\approx e^{B\,t_{\min}}$ where $t_{\min} = t_1 + \vec{p}_{3\perp}^{\,2} < 0$ and $B \sim 16\,\mathrm{GeV}^{-2}$ based on elastic scattering. A similar factor would be expected for the antiproton. However, this effect is found to be small enough to neglect in the region $X_1,\ X_2 > 0.95$.

Ordinary hard scattering generates a background to DPE that I estimate using a HERWIG QCD Monte Carlo simulation [28] in the manner described in Ref. [10]. The predicted cross section for two jets, each with $Q_\perp > 10\,\mathrm{GeV}$, in the DPE region defined by Eq. (33) is $30\,\mu\mathrm{b}$. This cross section is nearly four orders of magnitude larger than the signal. It is also nearly 10^{-3} of the entire minimum bias cross section, making it much too large to permit experiments to trigger on every such event.

Imposing a rapidity gap condition on *one side*, by requiring zero particles of transverse momentum $> 0.2\,\mathrm{GeV}$ in the range $\mathrm{Max}(\eta_5, \eta_6) + 0.7 < \eta < 4.2$, reduces the background by a factor 1/700. This makes it small enough to permit triggering on all such "single-gap" jet events.

Imposing a rapidity gap condition on *both sides* by requiring the regions $-4.2 < \eta < \mathrm{Min}(\eta_5, \eta_6) - 0.7$ and $\mathrm{Max}(\eta_5, \eta_6) + 0.7 < \eta < 4.2$ empty of particles with $p_\perp > 0.2\,\mathrm{GeV}$ leads to a HERWIG-predicted background cross section of 1.0 nb.

Our predicted cross section for quark jets alone is a factor of 5 larger than this background, so the DPE signal should show up clearly as an "extra" contribution at zero multiplicity in the particle multiplicity distribution for the gap regions of two-jet events. As a further test of the model, the DPE region could be tightened to $|\eta_5|$, $|\eta_6| < 1.0$ or < 0.5, which would increase the minimum rapidity gaps from 2.0 to 2.5 or 3.0. This would very strongly decrease the background from zero-multiplicity fluctuations of ordinary jet production. Of course, it would be better to extend the observed gap regions to larger $|\eta|$, or still better to detect the leading p and $\bar{p}$, but those options require additions to the detectors.

V. CONCLUSION

We have combined the two-gluon exchange model of the Pomeron with leading-order perturbative QCD for hard scattering to predict cross sections for $p\bar{p} \to p\bar{p}q\bar{q}$. The process shown in Fig. 3 gives the dominant contribution due to phase coherence of the sums over intermediate states represented by the hadronic discontinuities in Fig. 2.

A similar calculation of $p\bar{p} \to p\bar{p}gg$ is in progress. It is somewhat more complicated because many more diagrams make up the appropriate gauge-invariant set. The only anticipated difference from the $q\bar{q}$ result is that large rapidity separations will be possible between the jets, as a result of having spin 1 exchange in place of spin 1/2 between the jets. This could be observable at the LHC, but only by means of detectors with a wider coverage in pseudorapidity than those proposed so far. It cannot be observed at the Tevatron energy because jets with a large rapidity separation would have too large an invariant mass to be produced in the DPE region.

Our calculation resembles other QCD predictions, in that it contains a long distance scale nonperturbative part (the hadronic discontinuity which is related to a wave function), and a short distance scale (high-Q^2) part that is calculated perturbatively. It differs from other predictions, however, in that the nonperturbative part has been obtained by fitting to low-Q^2 elastic scattering rather than to a different high-Q^2 process, and in that there is no factorization theorem to guarantee success.

A special feature of this exclusive DPE process is that, unlike rapidity gaps created by other color singlet exchanges, there is presumably no additional "survival probability" factor needed to account for gaps that are filled in by incidental exchanges of color, e.g., due to additional soft gluons exchanged between the incident

beam particles. This is like elastic scattering itself. Of course, there will be some suppression due to the fact that soft particles from the jets can spread widely from the nominal jet axes. The effect of such particles can be reduced somewhat by defining gaps as an absence of particles above some threshold like $p_\perp > 0.2\,\mathrm{GeV}/c$ [10].

The experimental signature of our process is two hadronic jets separated by $\lesssim 2$ units of rapidity, and back-to-back in azimuthal angle. The final p and $\bar{p}$ are at such small angles with respect to the beam directions as to be undetectable in present experiments. Installing "Roman pot" detectors to cover the very small angle region would be valuable because it would easily eliminate all backgrounds to DPE, and because there are interesting correlations predicted between the transverse momenta of the two leading particles relative to each other and relative to the plane of the jets. In particular, the predicted cross section vanishes when both leading particles are at zero transverse momentum. This strongly contradicts a naive assumption of Regge factorization.

The predicted cross section for the $q\bar{q}$ process alone is $\sim 5\,\mathrm{nb}$. This is large enough to be studied easily at the Tevatron and at the eventual Large Hadron Collider at CERN. To make the study, it will be necessary to have an experimental trigger for the rapidity gap signature on at least one side of the detector. It will also be necessary to use sufficiently low luminosity running that the rapidity gaps are not filled in by particles from additional $p\bar{p}$ collisions that occur during the same beam crossing.

The production of jets discussed here is only one of many possible DPE processes, since $gg \to q\bar{q}$ could be replaced by any other hard scattering with a two-gluon initial state. Some suggestions are given in Ref. [5]. A further dramatic possibility would be DPE production of a Higgs boson [8, 12].

Some preliminary work on the subject of jet production in DPE was presented at the Fermilab Small-x Workshop [25, 29].

ACKNOWLEDGMENTS

I wish to thank my colleagues in the CTEQ Collaboration, especially J. Collins, H. Weerts, and S. Kuhlmann, for discussions. I also thank A. Berera, I. Balitsky, and V. Braun for useful discussions. I thank D. Zeppenfeld for pointing out the need to include the partially disconnected discontinuities in Fig. 3, which were neglected in an earlier version of this paper.

[1] F. Low, Phys. Rev. D **12**, 163 (1975); S. Nussinov, Phys. Rev. Lett. **34**, 1286 (1975); J. Gunion and D. Soper, Phys. Rev. D **15**, 2617 (1977).
[2] J. Pumplin and E. Lehman, Z. Phys. C **9**, 25 (1981); J. Pumplin, Phys. Rev. D **28**, 2741 (1983).
[3] A. Donnachie and P. V. Landshoff, Phys. Lett. B **296**, 227 (1992).
[4] P.V. Landshoff, in *Proceedings of the Summer School on Hadronic Aspects of Collider Physics*, Zuoz, Switzerland, 1994, edited by M. P. Locher (PSI, Villigen, 1994).
[5] J. Pumplin, Phys. Rev. D **47**, 4820 (1993).
[6] D. Joyce *et al.*, Phys. Rev. D **48**, 1943 (1993); M.G. Albrow, in *Elastic and Diffractive Scattering,* Proceedings of the International Conference, Evanston, Illinois, 1989, edited by M.M. Block and A.R. White [Nucl. Phys. B (Proc. Suppl.) **12**, 291 (1990)].
[7] A. Białas and W. Szeremeta, Phys. Lett. B **296**, 191 (1992); W. Szeremeta, Acta Phys. Pol. B **24**, 1159 (1993); A. Białas and R. Janik, Z. Phys. C **62**, 487 (1994).
[8] A. Schafer, O. Nachtmann, and R. Schopf, Phys. Lett. B **249**, 331 (1990); A. Białas and P.V. Landshoff, *ibid.* **256**, 540 (1991); B. Muller and A. Schramm, Nucl. Phys. **A523**, 677 (1991); R.S. Fletcher and T. Stelzer, Phys. Rev. D **48**, 5162 (1993); D. Zeppenfeld, talk given at 23rd International Symposium on Ultra-High Energy Multiparticle Phenomena, Aspen, Colorado, 1993 (unpublished).
[9] J.D. Bjorken, Int. J. Mod. Phys. A **7**, 4189 (1992); Phys. Rev. D **45**, 4077 (1992); **47**, 101 (1992); R.S. Fletcher, Phys. Lett. B **320**, 373 (1994).
[10] J. Pumplin, Phys. Rev. D **50**, 6811 (1994).
[11] A.H. Mueller and B. Patel, Nucl. Phys. **B425**, 471 (1994).
[12] H.-J. Lu and J. Milana, Phys. Rev. D **51**, 6107 (1995).
[13] M. Diehl, Z. Phys. C **66**, 181 (1995).
[14] E. Levin and M. Wusthoff, Phys. Rev. D **50**, 4306 (1994).
[15] S.J. Brodsky, L. Frankfurt, J.F. Gunion, A.H. Mueller, and M. Strikman, Phys. Rev. D **50**, 3134 (1994).
[16] K. Goulianos, in *Proceedings of the Workshop on Small-x and Diffractive Physics at the Tevatron*, Batavia, Illinois, 1994 (Fermilab, Batavia, 1994).
[17] J.C. Collins, L. Frankfurt, and M. Strikman, Phys. Lett. B **307**, 161 (1993).
[18] A. Berera and D.E. Soper, Phys. Rev. D **50**, 4328 (1994).
[19] G. Ingelman and P. Schlein, Phys. Lett. **152B**, 256 (1985).
[20] J. Collins, J. Huston, J. Pumplin, H. Weerts, and J. Whitmore, Phys. Rev. D **51**, 3182 (1995); J. Bartels and G. Ingelman, Phys. Lett. B **235**, 175 (1990); H.-J. Lu and J. Milana, *ibid.* **313**, 234 (1993); P. Bruni and G. Ingelman, *ibid.* **311**, 317 (1993); N. Nikolaev and B. G. Zakharov, Z. Phys. C **53**, 331 (1992); A. Donnachie and P.V. Landshoff, Phys. Lett. B **191**, 309 (1987); **198**, 590(E) (1987).
[21] UA8 Collaboration, A. Brandt *et al.*, Phys. Lett. B **297**, 417 (1992).
[22] M.B. Gay Ducati, F. Halzen, and A.A. Natale, Phys. Rev. **48**, 2324 (1993); F. Halzen, G.I. Krein, and A.A. Natale, *ibid.* **47**, 295 (1992); J.R. Cudell and B.U. Nguyen, Nucl. Phys. **B420**, 669 (1994); J.R. Cudell and B. Margolis, Phys. Lett. B **297**, 398 (1992).
[23] C. Bourrely, J. Soffer, and T.T. Wu, Z. Phys. C **37**, 369 (1988); Phys. Lett. B **252**, 287 (1990). For a discussion of this fit, see J. Pumplin, *ibid.* **276**, 517 (1992).
[24] UA4 Collaboration M. Bozzo *et al.*, Phys. Lett. **147B**, 385 (1984); **147B**, 392 (1984).
[25] A. Berera, in *Proceedings of the Workshop on Small-x and Diffractive Physics at the Tevatron* [16].
[26] A. Donnachie and P.V. Landshoff, Nucl. Phys. **B244**, 322 (1984); **B267**, 690 (1986); P.V. Landshoff and O.

Nachtmann, Z. Phys. C **35**, 405 (1987).
[27] S. Wolfram, MATHEMATICA (Addison-Wesley, Reading, MA, 1988, 1991).
[28] G. Marchesini and B.R. Webber, Nucl. Phys. **B310**, 461 (1988); G. Abbiendi, I.G. Knowles, G. Marchesini, B.R. Webber, M.H. Seymour, and L. Stanco, Comput. Phys. Commun. **67**, 465 (1992).
[29] J. Pumplin, in *Proceedings of the Workshop on Small-x and Diffractive Physics at the Tevatron* [16].